^{40}Ti β decay and the neutrino capture cross section of ^{40}Ar

W. Trinder, R. Anne, M. Lewitowicz, M.G. Saint-Laurent, C. Donzaud, D. Guillemaud-Mueller, S. Leenardt, a C. Mueller, F. Pougheon, O. Sorlin, et al.
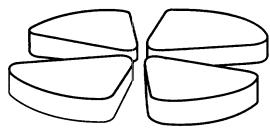
GANIL

^{40}Ti β decay and the Neutrino Capture Cross Section of ^{40}Ar

W. Trinder[a], R. Anne[a], M. Lewitowicz[a], M.G. Saint-Laurent[a], C. Donzaud[b],

D. Guillemaud-Mueller[b], S. Leenardt[b], A.C. Mueller[b], F. Pougheon[b], O. Sorlin[b],

M. Bhattacharya[c], A. García[c], N.I. Kaloskamis[c], E.G. Adelberger[d],

H.E. Swanson[d]

[a] GANIL, B.P. 5027, 14076 Caen Cedex 5, France,

[b] Institut de Physique Nucléaire, CNRS-IN2P3, 91406 Orsay Cedex, France,

[c] University of Notre Dame, Notre Dame, IN 46556, USA,

[d] University of Washington, Seattle, WA 98195, USA

^{40}Ti β decay and the Neutrino Capture Cross Section of ^{40}Ar

W. Trinder[a], R. Anne[a], M. Lewitowicz[a], M.G. Saint-Laurent[a], C. Donzaud[b],

D. Guillemaud-Mueller[b], S. Leenardt[b], A.C. Mueller[b], F. Pougheon[b], O. Sorlin[b],

M. Bhattacharya[c], A. García[c], N.I. Kaloskamis[c], E.G. Adelberger[d],

H.E. Swanson[d]

[a] *GANIL, B.P. 5027, 14076 Caen Cedex 5, France,*

[b] *Institut de Physique Nucléaire, CNRS-IN2P3, 91406 Orsay Cedex, France,*

[c] *University of Notre Dame, Notre Dame, IN 46556, USA,*

[d] *University of Washington, Seattle, WA 98195, USA*

Abstract: ^{40}Ti β decay was studied at GANIL using the LISE3 spectrometer. A decay scheme was deduced from twenty-one observed β-delayed proton transitions feeding the ground and first excited states of ^{39}Ca. The ^{40}Ti half-life was found to be 51.7(6) ms. These results imply that the ICARUS ^{40}Ar detector has an effective absorption cross section for ^{8}B solar neutrinos of 14.5(4)$\times 10^{-43}$ cm^2; 73% of the total cross section arises from Gamow-Teller transitions that were neglected in early estimates of the ICARUS efficiency.

The ICARUS large-volume liquid-argon time-projection chamber [1, 2] could provide useful information on the solar neutrino puzzle because it will detect neutrinos via $e^-(\nu_x, \nu_x)e^-$ scattering as well as via the $^{40}\mathrm{Ar}(\nu_e, e^-)^{40}\mathrm{K}$ neutrino capture reaction. Information about possible neutrino-flavour oscillations can be drawn from the *ratio* of scattering and absorption events, but definitive conclusions about neutrino properties are possible only if the detection efficiencies for the neutral and charged-current processes are well known. The cross sections for $e^- + \nu_x$ scattering as well as for the Fermi neutrino capture can be calculated accurately [3, 2]. However, the Gamow-Teller capture cross sections depend on model-dependent nuclear matrix elements. A recent shell-model calculation predicted that Gamow-Teller transitions contribute about 67% to the total $^{40}\mathrm{Ar}$ neutrino-capture cross section of $^8\mathrm{B}$ neutrinos [2] so that an empirical determination of the Gamow-Teller cross section is necessary for a reliable analysis of the ICARUS solar neutrino signals.

The transition strengths, $B(GT)$, for the Gamow-Teller absorption reactions in $^{40}\mathrm{Ar}$ can be deduced from the mirror β decays of $^{40}\mathrm{Ti}$. Under the assumption of isospin symmetry, the $B(GT)$ value for a $^{40}\mathrm{Ar}$ neutrino capture transition to an excited state of $^{40}\mathrm{K}$ is identical to the $B(GT)$ of the corresponding $^{40}\mathrm{Ti}$ β decay to the mirror state of $^{40}\mathrm{Sc}$. The large energy release in $^{40}\mathrm{Ti}$ decay assures that it can feed all states relevant for the Gamow-Teller contribution to the ICARUS signal. The single previous study of $^{40}\mathrm{Ti}$ decay [4] demonstrated that Gamow-Teller transitions play an important role in the $^{40}\mathrm{Ar}$ neutrino capture cross section, but statistical and systematic errors were not good enough to calibrate the ICARUS efficiency.

This letter describes a detailed study of the β-delayed proton emission of $^{40}\mathrm{Ti}$ to the ground and first excited states of $^{39}\mathrm{Ca}$ using the LISE3 spectrometer at GANIL [5]-[7]. A $^{40}\mathrm{Ti}$ secondary beam of about 0.3 atoms/s was produced by bombarding a 300 μm $^{nat}\mathrm{Ni}$ target with 82.6 A$\times$MeV $^{50}\mathrm{Cr}$ ions. The secondary beam purity was enhanced by a 215 μm $^9\mathrm{Be}$ degrader foil at the intermediate focal point and by the Wien velocity filter at the exit of LISE3. The $^{40}\mathrm{Ti}$ activity was implanted into a 500 μm silicon detector (implantation detector), which was

positioned between two similar silicon counters for registering β rays (β detectors). Two additional 300 μm silicon detectors, one of which was position sensitive, were mounted upstream; these provided energy-loss and time-of-flight for identifying the isotopes transmitted through the LISE3 spectrometer. Five large-volume (70%) germanium detectors mounted close to the silicon detector array registered γ rays.

A total of 6.3×10^4 ^{40}Ti atoms was collected in two different implantation modes of about equal statistics. In the first setting, the ^{40}Ti implantation profile (FWHM ≈ 50 μm) was centered a depth of about 100 μm and thus nearer to the upstream β detector. In the second setting, the profile was shifted to the center of the implantation detector by replacing one of the 300 μm detectors into a 150 μm one. In the following, we denote these modes as setting 1 and setting 2, respectively.

The secondary beam contained contaminating proton emitters (0.3 ^{41}Ti atoms/s and 0.04 ^{37}Ca atoms/s) along with a strong contribution of the β-emitter ^{38}Ca (0.7 atoms/s). Therefore, in analysing the proton spectrum we included only those ^{40}Ti events that were separated from preceeding ^{41}Ti or ^{37}Ca implantations by five respective half-lives *and* whose decay events occured before the arrival of the next ^{40}Ti, ^{41}Ti or ^{37}Ca atom. The proton-energy scale was calibrated by comparing our ^{41}Ti proton lines to those observed in a recent high-resolution study of ^{41}Ti β decay [8]. Corrections were made for the slightly different implantation depths of ^{40}Ti and ^{41}Ti ions ($\Delta \approx 20$ μm), and for the non-linear recoil defect [9]. The detection efficiency for high-energy protons was obtained from a Monte-Carlo simulation based on the measured implantation depth profile.

Figure 1a shows the raw proton spectrum of setting 2 and Fig. 1b the proton spectrum of setting 1 under the condition of a small energy loss of the coincident β rays in the upstream β detector ($\Delta E_\beta \leq 650$ keV). The resolution in the raw spectrum is poor because the continously distributed energy-loss of the coincident β ray was added to each proton signal. Spectrum 1b has much better resolution because its condition selects for events where the β rays leave little energy in the implantation detector (for more details about this technique see [10, 11]). In addition to the strong proton lines at 1.322, 1.698, 2.159 and 3.733 MeV that are

3

visible in both spectra, several weak lines were identified only in spectrum 1b. A small contamination of ^{41}Ti protons is indicated by the peak (marked with a star in spectrum b) from the proton decay of the ^{41}Sc isobaric analog state (IAS). Its intensity could be determined by varying the above mentioned selection conditions. Two weak low-energy proton lines were identified in spectrum c shown in the inset of Figure 1. Spectrum 1c shows the ^{40}Ti proton decay events of setting 2 with the requirement of a β ray in the upstream or downstream β detector with $\Delta E_\beta \leq 650$ keV. In addition, this spectrum contains only decays that occurred within one ^{40}Ti half-life (51.7(6) ms, see below) after the implantation of the corresponding ^{40}Ti atom. This decreased the ^{40}Ti statistics by a factor of two, but reduced the low-energy β background, mainly from ^{38}Ca decay, by a much larger factor.

We identified a total of twenty-one ^{40}Ti proton decay lines; the "line" at 4.353(99) MeV is an unresolved group of transitions. The energies of the proton groups and their absolute decay branching ratios, I_p, obtained by dividing the proton intensities by the number of implanted ^{40}Ti atoms (the latter were corrected for losses from secondary reactions in the stopping process [11]) are shown in Table 1, along with the low-statistics results of Détraz et al. [4]. When proton branching ratios were extracted under several β gating conditions the individual intensities of weak lines varied up to 2σ. However, the summed branches were consistent at 1σ level.

The γ ray signal in the germanium detectors was used to distinguish between β-delayed proton decays of ^{40}Ti to the ground (βp_0) and 2.469 MeV first excited state of ^{39}Ca (βp_1). The proton lines at 1.322(9) and 1.957(79) MeV were in coincidence with 2.469 MeV γ rays and identified as βp_1 transitions. The proton line at 1.574 MeV seemed to be coincident with Compton γ rays and was tentatively assigned to a βp_1 transition; β-proton decays of ^{40}Ti to other low-lying states in ^{39}Ca [12] are less probable for spin/parity reasons. Furthermore, $\beta\gamma$-proton decay is unlikely to compete significantly with βp_1 decay since the γ widths of highly unbound states are usually much smaller than their proton widths (the isospin-forbidden proton decay of the ^{40}Sc IAS could be an exception to this general expectation).

4

No conclusions could be drawn about the origins of the weak proton lines 1 and 2 in Table 1; the statistics of the coincident 2.469 MeV or Compton γ events were consistent with both βp_0 and βp_1 decay modes. Because the excitation energies of the ^{40}Sc 1^+ levels corresponding to the strong proton lines 5 and 7, 2.281(9) and 2.753(11) MeV, are close to the 1^+ ^{40}K states at 2.28988(3) and 2.73038(4) MeV [12], we identify these levels as isospin analogs. No other known or possible ^{40}K 1^+ levels occur in the well-studied region below 2.9 MeV. If lines 1 or 2 were due to βp_0 decays of ^{40}Ti, it would imply the existence of an unknown ^{40}K 1^+ level at low excitation energies or that the ^{40}Sc analog of the ^{40}K level at 2.28988 MeV was shifted downward by at least 0.6 MeV. Both possiblities are very unlikely. We therefore assigned these two lines to βp_1 decays. For all other ^{40}Ti proton lines, βp_1 decay could be excluded by the absence of the corresponding γ events.

The germanium detector spectrum in coincidence with β rays in the implantation detector showed no evidence for ^{40}Ti $\beta\gamma$ decays. From the β-signals in this counter an upper limit of 0.7% for the sum of all possible $\beta\gamma$-branchings could be extracted. Furthermore, no evidence was found for a possible $\beta\gamma$-proton decays of ^{40}Ti via the ^{40}Sc IAS. These isovector γ decays should have the same partial widths as the (bound) mirror IAS in ^{40}K [12] and therefore would feed ^{40}Sc states at 2.281 and 2.753 MeV with the subsequent emission of 1.698 and 2.159 MeV protons. The energies of the ^{40}Sc states and the absolute ^{40}Ti β-decay intensities I_β are shown in Table 2.

The ^{40}Ti half-life was extracted from the time differences between the stopped atoms and their subsequent decay events. A background of β rays or fast charged particles penetrating all three detectors was excluded by a two-dimensional condition on proton energy versus the β-detector signals. Corrections were made for a small background in the time spectrum arising from ^{40}Ti, ^{41}Ti or ^{37}Ca decay events where the arrival of the corresponding atom was missed for dead-time reasons, and for events where a second heavy ion closed the correlation gate *before* the first ion had decayed. The resulting ^{40}Ti half-life of 51.7(6) ms can be compared with the previous value 56^{+18}_{-12} ms [4]. Our ^{41}Ti half-life, 80.1(9) ms, agrees with the previous, less precise, value of 80(2) ms [13].

5

The β-decay transition strengths were computed using the relation

$$(B(F) + B(GT))_i = \frac{K}{f(E_i)t_i}$$

where $B(F)$ is the Fermi strength, $K = 6127(9)$ s [17], and E_i, t_i and $f(E_i)$ are the β-endpoint energy, the partial half-life and the phase-space factor [18], respectively, of a β transition to state i in ^{40}Sc. The phase space factor is a strong function of the energy release in the decay, the uncertaintly of which is dominated by the ± 160 keV uncertainty in the ^{40}Ti mass [14, 16]. We finessed this problem by using the isobaric multiplet mass equation (IMME) to predict the ^{40}Ti mass from the precisely known masses of the other four members of the lowest lying A = 40, T = 2 multiplet. The mass excess of the $T_z = -1$ member, $-16160.8(9.2)$ keV, determined from our measured excitation energy of the IAS in ^{40}Sc, agrees well with the quadratic IMME prediction $-16161.2(6.1)$ keV. From the mass excesses of the $T_z = 2, 1, 0$, and -1 members, $-35039.890(4)$, $-29151.0(4)$, $-22858.1(2.0)$, and $-16160.8(9.2)$ keV [12, 14] respectively, we predict a ^{40}Ti mass excess of $-9060(12)$ keV. Because, as shown in Table 3, the quadratic IMME provides an excellent fit to the well-known multiplet masses ($\chi^2/\nu = 1.19$, $P(\chi^2, \nu) = 0.30$), we conclude that the measured ^{40}Ti mass excess, $-8850(160)$ keV, is off by about 1.3σ, and deduce from the IMME equation an electron capture Q value of $11466(13)$ keV for ^{40}Ti decay to the ground state of ^{40}Sc. The resulting $B(F) + B(GT)$ values are shown in Table 2.

The observed strength, $B(F) = 3.90(25)$, of the pure Fermi transition to the 4.365(8) MeV IAS agrees well with the model-independent value $B(F) = |Z - N| = 4$, providing an impressive overall check on our absolute β-decay branching ratios. It is possible that part of the Fermi strength is mixed into $J^\pi = 0^+$; $T = 1$ states that may lie close to the IAS [2]. Because we cannot exclude the possibility that the ^{40}Sc state at 4.265(22) MeV is a 0^+, $T = 1$ level fed in a isospin-forbidden Fermi transition carrying 5% of the total Fermi strength, we give this level a $J^\pi = (0, 1)^+$ assignment. The strengths of the transitions to the remaining states indicate allowed transitions and hence 1^+ assignments.

Figure 2 compares our integrated ^{40}Ti GT strength as a function of excitation

energy in ^{40}Sc to the shell-model calculation [2]. The *shape* of the integrated strength is well reproduced by the theory, but the theoretical excitation energies are generally about 0.5-1.0 MeV too high; a similar failure has been been observed in ^{37}Ca decay [19]. Furthermore, the strength is spread over more levels than predicted by the theory, especially around $E_x = 3$ MeV. This is presumably due to higher-order correlations neglected in the model; these can fragment the GT strength without significantly changing its magnitude.

The ICARUS detector is expected to have an electron energy threshold of $W = 5$ MeV for charged-current capture events [1]. The capture cross-section of ^{8}B neutrinos on ^{40}Ar, with this threshold on the outgoing electron, was calculated following the procedure described in Ref. [2] except that the ^{8}B neutrino spectrum of [20] was used. Cross sections were computed using the ^{40}K excitation energies [12] for the IAS and the lowest two 1^{+} states (see Table 2). We could not find definitive ^{40}K analogs for the remaining ^{40}Sc daughters fed in ^{40}Ti decay, and were forced to use ^{40}Sc energies in those cases. However, the uncertainty introduced by this approximation is very small as these remaining transitions account for only 21% of the total cross section and the excitation energy shifts are likely to be only some tens of keV. We used the measured B value for the ^{40}Ar capture rate into the IAS in ^{40}K instead of the theoretical value $B(F) = 4$. The actual B value could well be less than 4 (if isospin mixing removed some of the Fermi strength) or exceed 4 (if a Gamow-Teller transition to a 1^{+} level were not resolved from the Fermi transition to the IAS). The resulting ^{40}Ar neutrino cross sections for ^{8}B neutrinos, along with the $B(F) + B(GT)$ values used in the computation are shown in Table 2.

The sum of the cross sections is $14.5(4) \times 10^{-43}$ cm^2, about 73% of which arises from Gamow-Teller transitions. Ormand *et al.* predicted a cross section of $11.5(7) \times 10^{-43}$ cm^2. As can be seen from Figure 2, much of the discrepancy between experiment and theory is due to the failure of the theory to reproduce the excitation energies. Our ^{40}Ar cross section for absorbing ^{8}B neutrinos corresponds to a neutrino capture rate of $9.6^{+1.4}_{-1.7}$ SNU [21].

In summary, we have used the mirror β decay of ^{40}Ti to obtain an empirical

value for the ^{40}Ar cross section for absorbing ^{8}B neutrinos. About 73% of the ^{40}Ar neutrino capture rate arises from Gamow-Teller transitions. This increases the charged-current efficiency of the ICARUS detector over the original prediction which assumed that the cross section was dominated by the Fermi transition. A more detailed discussion of the results will be presented elsewhere [22].

References

[1] ICARUS Collaboration, ICARUS II Proposal (1993), *A second-generation proton decay experiment and neutrino observatory at the Gran Sasso Laboratory.*

[2] W.E. Ormand et al., Phys. Lett. B345 (1995) 343.

[3] J.N. Bahcall et al., Phys. Lett. B178 (1986) 324.

[4] C. Détraz et al., Nucl. Phys. A519 (1990) 529.

[5] R. Anne et al., Nucl. Instr. Meth. A257 (1987) 215.

[6] A.C. Mueller and R. Anne, Nucl. Instr. Meth. B56/57 (1991) 559.

[7] R. Anne and A.C. Mueller, Nucl. Instr. Meth. B70 (1992) 276.

[8] A. Honkanen et al., Nucl. Phys. A, in print.

[9] C. Chasman et al., Phys. Rev. Lett. 15 (1965) 245.

[10] A. Piechaczek et al., Nucl. Phys. A584 (1995) 509.

[11] W. Trinder, Ph.D. thesis, Universität Frankfurt a.M. (1995).

[12] P.M. Endt, Nucl. Phys. A521 (1990) 1.

[13] R.G. Sextro et al., Nucl. Phys. A234 (1974) 130.

[14] G. Audi and A.H. Wapstra, Nucl. Phys. A595 (1995) 409.

[15] M.S. Antony et al., At. Data Nucl. Data Tables 33 (1985) 447.

[16] C.L. Morris et al., Phys. Rev. C25 (1982) 3218.

[17] D.H. Wilkinson, Nucl. Instr. Meth. A335 (1993) 172, 201.

[18] D.H. Wilkinson and B.E.F. Macefield, Nucl. Phys. A232 (1974) 58.

[19] N.I. Kaloskamis et al., Phys. Rev. C55 (1997) 630.

[20] J.N. Bahcall and B.R. Holstein, Phys. Rev. C33 (1986) 2121.

[21] J.N. Bahcall et al., Rev. Mod. Phys. 67 (1995) 781.

[22] M. Bhattacharya et al., to be published.

Table 1: Absolute β-delayed proton intensities in ^{40}Ti decay.

Line	E_p(MeV) this work	I_p	E_p(MeV) ref. [4]	I_p
(1	0.709(25)	0.0034(10))		
2	1.105(26)	0.0031(11)		
3	1.322(9)	0.0346(25)		
4	1.574(28)	0.0045(12)		
5	1.698(9)	0.249(7)	1.84(12)	0.04(2)
6	1.957(79)	0.013(2)		
7	2.159(10)	0.294(14)	2.24(12)	0.20(4)
8	2.355(35)	0.0086(22)		
9	2.481(26)	0.016(3)	2.56(12)	0.03(1)
10	2.708(31)	0.016(3)		
11	2.902(31)	0.013(3)		
12	3.046(23)	0.018(3)		
13	3.153(20)	0.029(4)		
14	3.428(35)	0.011(2)		
15	3.633(21)	0.0099(18)		
16	3.733(12)	0.218(15)	3.84(12)	0.16(4)
17	3.890(33)	0.014(3)		
18	4.015(32)	0.015(4)		
19	4.353(99)	0.02(1)		
20	4.951(60)	0.0063(20)		
21	5.308(33)	0.0068(20)		
TOTAL		1.002(26)		0.43(6)

Table 2: β decays of ^{40}Ti and their isobaric-analog neutrino captures on ^{40}Ar. Excitation energies are given in MeV. The neutrino capture cross sections assume a 5 MeV threshold on the total energy of the outgoing electron; the incoming neutrinos are assumed to have the standard ^{8}B spectrum.
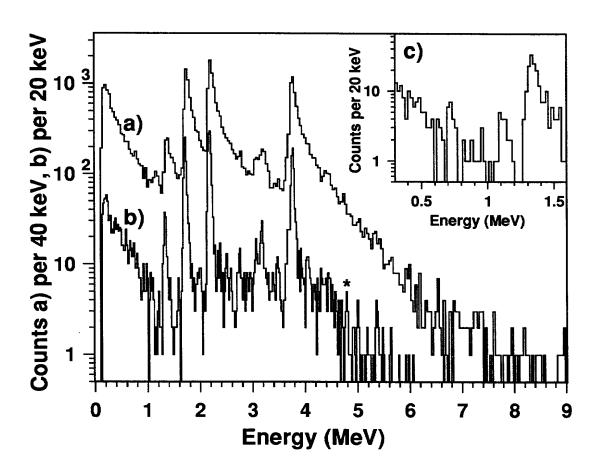
i	^{40}Ti decay					^{40}Ar(ν, e)	
	$E_i(^{40}$Sc$)$	decay	J^π	I_β	$B(F) + B(GT)$	$E_i(^{40}$K$)$	$\sigma_\nu(10^{-43}\text{cm}^2)$
1	2.281(9)	p_0	1^+	0.249(7)	0.96(3)	2.290	3.40(10)
2	2.753(11)	p_0	1^+	0.294(14)	1.50(7)	2.730	4.22(21)
3	2.955(35)	p_0	1^+	0.0086(22)	0.050(13)	(3.110)	0.12(3)
4	3.084(26)	p_0	1^+	0.016(3)	0.101(17)		0.23(4)
5	3.317(31)	p_0	1^+	0.016(3)	0.114(20)		0.23(4)
6	3.515(31)	p_0	1^+	0.013(3)	0.105(23)		0.19(4)
7	3.664(23)	p_0	1^+	0.018(3)	0.16(3)		0.26(5)
8	3.758(20)	p_0, p_1	1^+	0.032(5)	0.32(5)		0.49(7)
9	4.055(35)	p_0	1^+	0.011(2)	0.14(3)		0.17(3)
10	4.141(26)	p_1	1^+	0.0031(11)	0.040(14)		0.047(17)
11	4.265(22)	p_0	$(0,1)^+$	0.0099(18)	0.14(3)		0.15(3)
12	4.365(8)	p_0, p_1	0^+	0.252(16)	3.90(25)	4.384	3.87(25)
13	4.528(33)	p_0	1^+	0.014(3)	0.24(6)		0.21(5)
14	4.637(29)	p_0, p_1	1^+	0.020(4)	0.38(8)		0.30(6)
15	5.003(99)	p_0, p_1	1^+	0.056(6)	0.9(3)		0.48(15)
16	5.617(61)	p_0	1^+	0.0063(20)	0.28(9)		0.09(3)
17	5.983(33)	p_0	1^+	0.0068(20)	0.44(13)		0.10(3)

Table 3: Coefficients of the IMME for the lowest $T = 2$ multiplet in $A = 40$.

a (keV)	b (keV)	c (keV)	d (keV)	e (keV)	χ^2/ν	P(χ^2/ν)
−22857.9(1.6)	−6495.2(2.4)	202.1(8)			1.19	0.30
−22858.3(2.5)	−6495.8(4.1)	203.7(6.2)	−0.6(2.3)		2.28	0.13
−22858.1(2.6)	−6495.8(6.0)	203.0(7.7)		−0.1(1.2)	2.36	0.12
−22858.1(2.0)	−6478(15)	194(9)	−17(13)	9(7)		

Figure 1: Delayed proton spectra from ^{40}Ti β decay. Panel a shows the raw spectrum at setting 2 while panel b shows the β-coincident spectrum at setting 1. The inset (spectrum c) is part of the β-coincident spectrum of setting 2, but with the requirement of a short decay-time window (see text). The energy scale refers to the detector signal (decay energy minus recoil loss); the mean shift due to β summing has been subtracted.

Figure 2: Comparison of the integrated $B(GT)$ strength (solid lines indicating the $\pm 1\sigma$ uncertainty band) with a shell-model calculation [2] (dashed line).

Integrated Gamow-Teller strength

Excitation energy in ^{40}Sc (MeV)